

Athermal laser design

Jock Bovington,* Sudharsanan Srinivasan, and John E. Bowers

Department of Electrical & Computer Engineering, University of California Santa Barbara, California, USA

*jock@ece.ucsb.edu

Abstract: This paper discusses circuit based and waveguide based athermalization schemes and provides some design examples of athermalized lasers utilizing fully integrated athermal components as an alternative to power hungry thermo-electric controllers (TECs), off-chip wavelength lockers or monitors with lookup tables for tunable lasers. This class of solutions is important for uncooled transmitters on silicon.

©2014 Optical Society of America

OCIS codes: (140.3425) Laser stabilization; (140.6810) Thermal effects; (160.6840) Thermo-optical materials; (130.3120) Integrated optics devices.

References and links

1. H. Tanobe, Y. Kondo, Y. Kadota, H. Yasaka, and Y. Yoshikuni, "A temperature insensitive InGaAsP-InP optical filter," *IEEE Photon. Technol. Lett.* **8**(11), 1489–1491 (1996).
2. H. Tanobe, Y. Kondo, Y. Kadota, K. Okamoto, and Y. Yoshikuni, "Temperature insensitive arrayed waveguide gratings on InP substrates," *IEEE Photon. Technol. Lett.* **10**(2), 235–237 (1998).
3. J. Teng, P. Dumon, W. Bogaerts, H. Zhang, X. Jian, X. Han, M. Zhao, G. Morthier, and R. Baets, "Athermal Silicon-on-insulator ring resonators by overlaying a polymer cladding on narrowed waveguides," *Opt. Express* **17**(17), 14627–14633 (2009).
4. J. Bovington, R. Wu, K. T. K.-T. Cheng, and J. E. J. E. Bowers, "Thermal stress implications in athermal TiO₂ waveguides on a silicon substrate," *Opt. Express* **22**(1), 661–666 (2014).
5. S. S. Djordjevic, K. Shang, B. Guan, S. T. S. Cheung, L. Liao, J. Basak, H.-F. Liu, and S. J. B. Yoo, "CMOS-compatible, athermal silicon ring modulators clad with titanium dioxide," *Opt. Express* **21**(12), 13958–13968 (2013).
6. B. Guha, J. Cardenas, and M. Lipson, "Athermal silicon microring resonators with titanium oxide cladding," *Opt. Express* **21**(22), 26557–26563 (2013).
7. D. Bosc, B. Loisel, M. Moisan, N. Devoldere, F. Legall, and A. Rolland, "Temperature and polarisation insensitive Bragg gratings realised on silica waveguide on silicon," *Electron. Lett.* **33**(2), 134–136 (1997).
8. R. R. Alexander, D. T. D. Childs, H. Agarwal, K. M. Groom, H. Liu, M. Hopkinson, R. A. Hogg, M. Ishida, T. Yamamoto, M. Sugawara, Y. Arakawa, S. Member, T. J. Badcock, R. J. Royce, and D. J. Mowbray, "Systematic study of the effects of modulation p-doping on 1.3- μm quantum-dot lasers," *IEEE J. Quantum Electron.* **43**(12), 1129–1139 (2007).
9. A. Y. Liu, C. Zhang, J. Norman, A. Snyder, D. Lubyshev, J. M. Fastenau, A. W. K. Liu, A. C. Gossard, and J. E. Bowers, "High performance continuous wave 1.3 μm quantum dot lasers on silicon," *Appl. Phys. Lett.* **104**(4), 041104 (2014).
10. M. T. Crowley, GaAs based Quantum Dot Lasers, *Semiconductors and Semimetals: Advances in Semiconductor Lasers*, 86, (2012).
11. D. A. Cohen, M. E. Heimbuch, and L. A. Coldren, "Reduced temperature sensitivity of the wavelength of a diode laser in a stress-engineered hydrostatic package," *Appl. Phys. Lett.* **69**(4), 455 (1996).
12. A. Phillips, R. Penty, and I. White, "Integrated passive wavelength athermalisation for vertical-cavity semiconductor laser diodes," *Optoelectron. IEEE Proc.*, 152(3), (2005).
13. H. Park, M. Sysak, H. Chen, A. W. Fang, D. Liang, L. Liao, B. R. Koch, J. Bovington, Y. Tang, K. Wong, M. Jacob-Mitos, R. Jones, and J. E. Bowers, "Device and Integration Technology for Silicon Photonic Transmitters," *IEEE J. Sel. Top. Quantum Electron.* **17**(3), 671–688 (2011).
14. B. Liu, A. Shakouri, and J. E. Bowers, "Passive microring-resonator-coupled lasers," *Appl. Phys. Lett.* **79**(22), 3561 (2001).

1. Introduction

Athermal devices are needed as a method of reducing the single lane guard band of uncooled interconnects. Uncooled wavelength division multiplexing (WDM) interconnects are the clear choice for reasons of energy efficiency to address the exponential growth of demand for bandwidth. At this time new solutions are required. Bandwidth demands for a given range of

wavelengths, typically a single laser gain medium bandwidth, can be met by either an increase in the number of symbols per bit of a single channel or by decreasing the channel spacing, or some combination of the two. Figure 1 illustrates the trade-off as normalized to a 10Gbps non-return to zero (NRZ) signal. Typically the energy cost of digital signal processing for anything beyond the simplest of higher order modulation schemes would tend to bias a designer to pursue denser channel spacing before advanced modulation. However, this requires that one address the thermal drift challenge. Figure 1 assumes the spectral efficiency of higher order modulation signals scales linearly with channel spacing and modulation order as a first order approximation, a similar trade-off exists at higher baud rates.

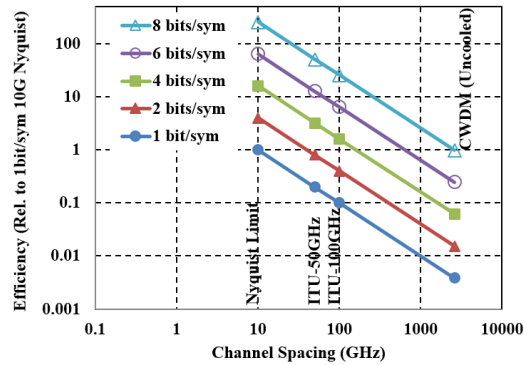


Fig. 1. Normalized spectral efficiency v. channel spacing for various higher order modulations assuming a linearly proportional model.

In this paper we explore the concept of an athermal laser as part of the solution to this problem. Tunable lasers are also a potential solution, however the feedback schemes required to stabilize them are more complicated than the approaches proposed here or require the additional complexity of an off-chip filter and monitor (wavelength locker) or on-chip temperature sensor and lookup table with associated memory and logic. The following sections include a brief background of the concepts and technologies that enable these novel designs and a few examples of designs that meet the requirements of uncooled WDM laser sources.

2. Background and theory on athermal technologies

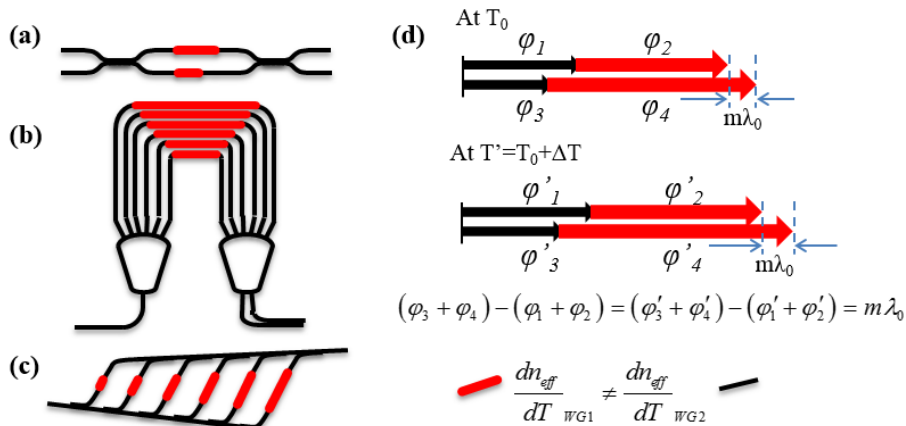


Fig. 2. (a-c) Three FIR filters whose response can be made less sensitive to temperature variation by using two waveguide types (shown in red and black) each with a different thermo-optic coefficient. (d) Vector representation of effective path length for circuit (a) showing the principle whereby the phase difference of the paths is constant with temperature (T and T').

The simplest athermal technology is the athermal waveguide. Such waveguides can be broken into athermal circuit-based guides and materials-based guides. Circuit based guides have been used to create finite impulse response (FIR) filters where the temperature sensitivity of the center wavelength is reduced significantly [1,2]. Some of the common FIR filters that can be made athermal are shown in Fig. 2. The main design methodology used in these structures is that the filter response depends only on the phase difference between the interfering waveguides and not the absolute phase shift. By co-integrating waveguides with different thermo-optic coefficients, and adjusting the length of each waveguide type, the phase difference between the neighboring waveguides can in principle be independent of temperature, over a range in excess of 50°C [1,2]. The same principle does not apply to the case of infinite impulse response (IIR) filters like ring resonators and Bragg gratings as the filter response depends on the absolute phase shift, which significantly reduces the temperature range over which they can be compensated using the same technique. Also the filter shape and insertion loss would vary thereby forming a limitation to circuit based techniques to create IIR filters.

Given the limitations of circuit based athermalization, materials based athermalization is an important addition. In essence, materials based athermalization as described with reference to Eqs. (1) and (2), is achieved by engineering a waveguide with k (two or more) materials and balancing their confinement factor, Γ , with their material thermo-optic coefficient, dn_k/dT , such that the thermal drift $d\lambda_r/dT$ is close to zero. Here n_{eff} , n_g and α_{sub} are the effective and group index of the mode and the linear thermal expansion coefficient of the substrate, which is assumed to dominate the thermal expansion of the optical path length.

$$\frac{d\lambda_r}{dT} \approx \frac{\lambda_r}{n_g} \left(n_{eff} \alpha_{sub} + \frac{\partial n_{eff}}{\partial T} \right) \quad (1)$$

$$\text{where, } \frac{\partial n_{eff}}{\partial T} \approx \sum_k \Gamma_k \frac{\partial n_k}{\partial T}. \quad (2)$$

For a number of years, polymer based materials have been used for athermalization because of their negative thermo-optic coefficient [3]. However, these materials are not always compatible with other processes, and suffer from degradation over time and/or in harsh environments. TiO₂ is a more recent choice for a potentially CMOS compatible material alternative. The most commonly reported athermal structures have been rings as they act as a convenient diagnostic structure for probing the waveguide and material parameters through Eqs. (1) and (2). Demonstrations have been made with athermalized rings [4–6], ring modulators [5] and DBR gratings [7], which add more functional elements for a WDM link.

In order to athermalize a laser, one must carefully design for thermal drift of gain, loss, and cavity modes. Figure 3 shows a diagram of these three effects and provides typical values from thermal drift in semiconductor lasers with semiconductor mirrors. In general for an in-plane DBR, the thermal drift is represented by Eq. (3). This is an approximation for 50% duty cycle gratings and is similar to Eq. (1) utilizing the same definition in Eq. (2) for dn_{eff}/dT .

$$\frac{d\lambda_{Bragg}}{dT} \approx \frac{1}{m} \frac{\lambda_{Bragg}}{n_{g1} + n_{g2}} \left[(n_{eff1} + n_{eff2}) \alpha_{sub} + \frac{dn_{eff1}}{dT} + \frac{dn_{eff2}}{dT} \right] \quad (3)$$

In Eq. (3) λ_{Bragg} is the Bragg wavelength, or first order peak reflection wavelength, m is the order of the grating, $n_{g1,2}$ and $n_{eff1,2}$ are the group and effective indices corresponding to the two periodically repeating segments of the grating.

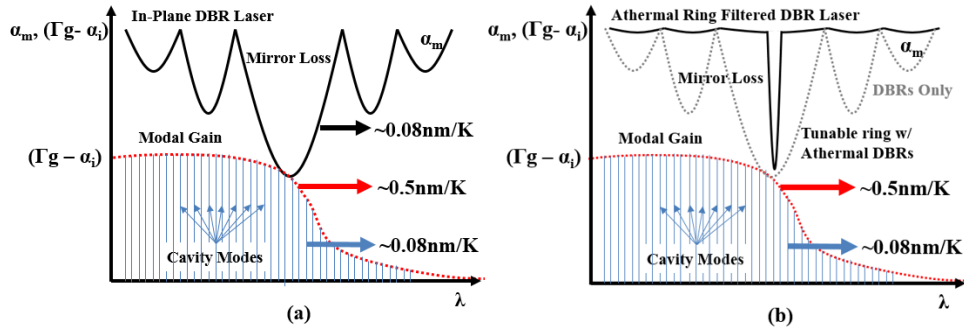


Fig. 3. (a) Diagram of typical in-plane semiconductor laser with dense cavity modes where thermal drift is typically dominated by cavity loss. (b) A similar DBR laser design with and intra-cavity ring filter to achieve a narrower reflectivity bandwidth.

Thermal drift in gain is challenging to athermalize for because it is so fundamental to the change in band gap of the semiconductor gain material with respect to temperature. The two examples that perhaps have done the best job of overcoming this limitation are p-doping of quantum dots which can result in negligible change in threshold current with temperature or $T_0 = \infty$ at low temperatures and as much as 120K up to 85°C [8–10], and the induction of hydrostatic pressure as a means to automatically counteract the typical thermal effect on the band gap and thus gain peak wavelength [11].

Thermal drift in loss is typically manifest in the most spectrally sharp loss of the cavity, the mirror. For in-plane lasers with integrated DBR mirrors this drift, though it doesn't drift as rapidly as the gain peak, is the single most significant factor in laser wavelength drift. In contrast, in short cavity lasers such as vertical cavity surface emitting lasers, (VCSELs) cavity mode drift is often the most significant. Athermalized VCSEL designs which modify the cavity with polymers and air gaps to compensate for cavity mode drift have already been proposed by Phillips et al. [12]. Our work focuses on in-plane devices and therefore athermalization must be made both in the mirror and the cavity.

3. Examples of integrated athermal lasers

One typical solution to temperature variations in uncooled WDM transmitter has been to use a tunable laser locked to an external wavelength locker, which varies only slightly with temperature or is itself regulated by a TEC. However, in this work we propose some designs which require no or only minimal laser feedback such that all lasers in an array can be easily integrated together with a channel spacing considerably less than the 20nm specification of conventional uncooled coarse WDM.

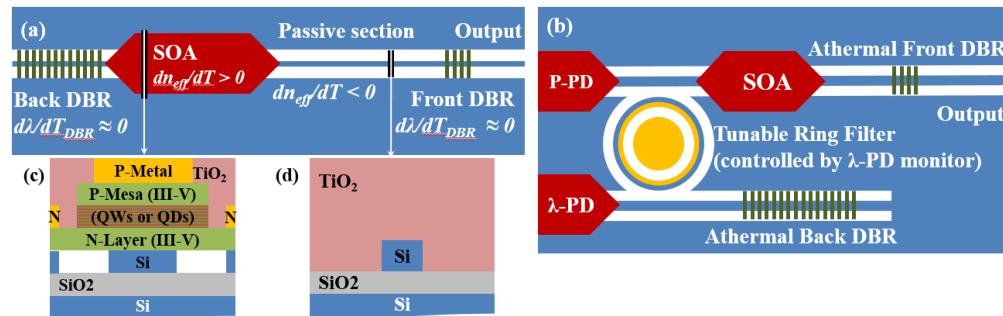


Fig. 4. (a) Passively Athermal DBR Laser (b) Athermal Ring Filtered DBR (ARF-DBR) Laser (c) cross section of III-V/Si Hybrid SOA or PD with TiO₂ cladding. (d) cross section of Si waveguide clad with TiO₂ for a thermal compensator.

Figure 4(a) shows a passively athermal DBR laser cavity, the simplest manifestation of an integrated athermal laser requiring no tuning or feedback. The principle is that the cavity mode thermal drift is managed by cavity design following Eq. (4) and the mirror thermal drift is managed by creating an athermal DBR mirror design following Eq. (3). The gain drift is not compensated for, but rather the bandwidth of the gain can and must be wide enough to function across the entire temperature range of the application space. Thermal roll-off via self-heating can also be partially accounted for either by selection of a high T_0 material such as QDs or by simply aligning the low temperature lasing wavelength on the long wavelength side of the gain peak, as shown in Fig. 3(a) such that heating will push the gain peak towards the minimum loss wavelength of the athermal mirror decreasing the threshold before it increases again at the high temperature range of operation where the gain drops. This method of gain offsetting is a common technique utilized in current uncooled VCSELs.

$$\frac{d\lambda_c}{dT} \approx \frac{\lambda_c}{\int_{L_c} n_g dL} \left(\alpha_{sub} \int_{L_c} n_{eff} dL + \int_{L_c} \frac{dn_{eff}}{dT} dL \right) \quad (4)$$

Equation (4) represents cavity mode drift $d\lambda_c/dT$ for an FP laser or similar laser with broadband mirrors and multiple sections. The integrations are done over a single round trip laser path length, L_c , of the modal properties n_g , n_{eff} , and dn_{eff}/dT . Finding the criteria that upholds the condition $d\lambda_c/dT = 0$ is possible by use of a waveguide section with a negative TO

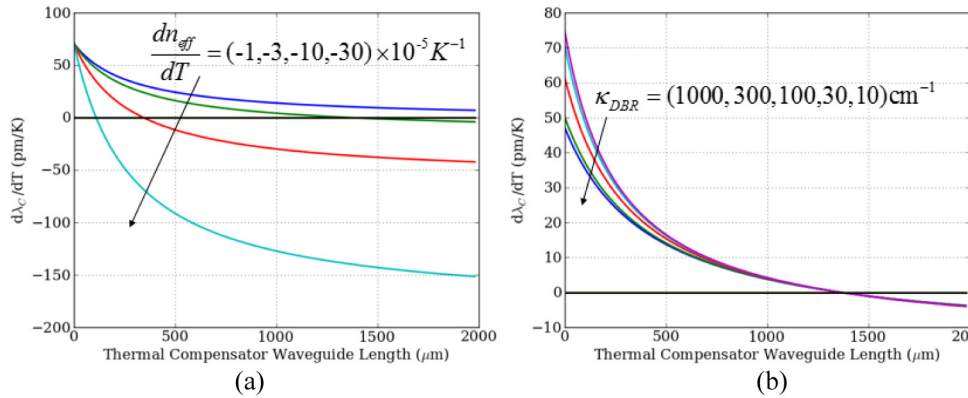


Fig. 5. Athermal DBR laser drift in pm/K vs. the length of a thermal compensator waveguide as a function of (a) different passive compensator drifts dn_p/dT and (b) athermal grating strengths κ_{DBR} . Hybrid silicon gain region length assumed to be $200\mu\text{m}$ with compensator made of a Si core with TiO_2 cladding, and $250\mu\text{m}$ combined grating length for front and back. (a) assume $\kappa_{DBR} = 300\text{cm}^{-1}$, (b) assumes $dn_p/dT = -3 \times 10^{-5}\text{K}^{-1}$.

coefficient if its length is appropriately weighted with the sections of the laser that have a positive thermo-optic coefficient, such as the semiconductor gain region. Figure 5 plots the wavelength drift as an example. Assuming that any additional packaging required to offset the gain's band gap change with hydrostatic pressure or other such methods are prohibitive, it is appropriate to use conventional semiconductor parameters. The platform selected for this example is the Hybrid Silicon Laser Platform [13] with a modification where TiO_2 cladding is added as an alternative to SU-8. Therefore with a single lithography, the waveguide width of the passive section with $dn_{eff}/dT < 0$ and the DBR section with $d\lambda_{DBR}/dT \approx 0$ can be integrated. Using the model based on data collected by Guha et al. [5] at 1550nm on 220nm SOI, a 200nm wide waveguide with 500nm of TiO_2 shows a $d\lambda/dT = -20\text{pm/K}$, and a 270nm waveguide guide is nearly athermal. The 200nm guide results in a dn_{eff}/dT for the negative TO

compensation guide of $\sim -4.3 \times 10^{-5}/\text{K}$. This is compared to dn_{eff}/dT for the gain section of $\sim 2 \times 10^{-4}/\text{K}$ or a ratio of just under 5 in length for the gain to negative TO waveguide. Therefore, for short gain lengths possible on the Hybrid Silicon Laser Platform, the total cavity length need not be greater than 1mm provided a strong negative TO guide is available in the platform, as seen in Fig. 5. An issue does arise when using DBR lasers that are $\sim 1\text{mm}$ long, which is that the FSR or the cavity is $\sim 0.4\text{nm}$, stipulating that to get a grating stop bandwidth on the order of the free spectral range of the cavity to avoid mode hopping requires a grating strength $\sim 10\text{cm}^{-1}$.

$$\frac{dL_{eff}}{dT} \approx \frac{\alpha_{sub} L_g}{2} \operatorname{sech}^2 \left(\frac{2\delta L_g}{\lambda_0} \right) - \frac{L_g}{\delta} \frac{d\delta}{dT} \left(1 - \frac{\lambda_0}{2\delta L_g} \tanh \left(\frac{2\delta L_g}{\lambda_0} \right) \right) \quad (5)$$

However, the length of the grating for appropriate reflectivity would then be such that the cavity length itself would grow considerably as the effective grating length, L_{eff} , would become significant to the total cavity length. This is important as dL_{eff}/dT is proportional to the grating length L_g as shown in Eq. (5) where δ is simply the difference in effective indices of the two periodic grating sections n_{eff1} and n_{eff2} . The $L_{eff} \rightarrow L_g$ case is not shown in Fig. 5, which has fixed grating lengths of $250\mu\text{m}$ for all curves. This logical progression implies that ideally the platform best suited to this design is one that has not been created yet to utilize active III-V integration on waveguides both capable of highly negative and athermal TO drift. For example TiO_2 core guides demonstrated with both $\sim -100\text{pm}/\text{K}$ and $< -3\text{pm}/\text{K}$ drift [4]. Alternatively, if narrow FSRs with these thermally compensated lasers are not avoidable, an intracavity filter should be used, as discussed below and shown in Fig. 4(b).

Plotted in Fig. 5 is the trade-off of the athermal compensator waveguide length with the choice of compensator waveguide and grating design. Figure 4(c) shows that less than 1.5mm of compensator waveguide is required if a 200nm wide Si with TiO_2 cladding is used ($dn_{eff}/dT \approx -3 \times 10^{-5}/\text{K}$). Alternatively, using a waveguide such as the TiO_2 core guide in [4] has been demonstrated with $dn_{eff}/dT \approx -17.5 \times 10^{-5}/\text{K}$ which would reduce the required compensator length to $\sim 300\mu\text{m}$ for an athermal design. Figure 5(b) shows little impact of grating strength with selection of the compensator length.

Figure 4(b) shows an ARF-DBR utilizing a ring resonator as an intracavity filter, an athermal variation of a previous concept [14]. If the design of the passive straight waveguides of the laser is such that they compensate the positive TOC of the SOA as in the athermal DBR example, then this filter can be athermal as cavity modes will not drift out of the filter. However, as precisely aligning the cavity modes to the resonance of the ring may prove to be beyond fabrication tolerances, a simple feedback scheme can be utilized to maximize power to the wavelength monitor photo-diode, λ -PD, by tuning the intracavity ring filter so the lasing mode is centered about the rear athermal DBR. A number of feedback schemes would suffice here, for example a proportional-integral-derivative (PID) controller. The power monitor photodiode, P-PD, also is in a simple feedback with the SOA bias to regulate the output power of the laser out of the front facet without tapping the signal power at the output of the cavity. Of course one can still tap the actual output with an additional monitor PD, but this utilizes an existing port in the architecture and will act as a fair and representative signal in most regimes of SOA operation, which is already constrained by the lasing condition.

A ring filter is needed as the cavity length of a standard DBR reduces the free-spectral

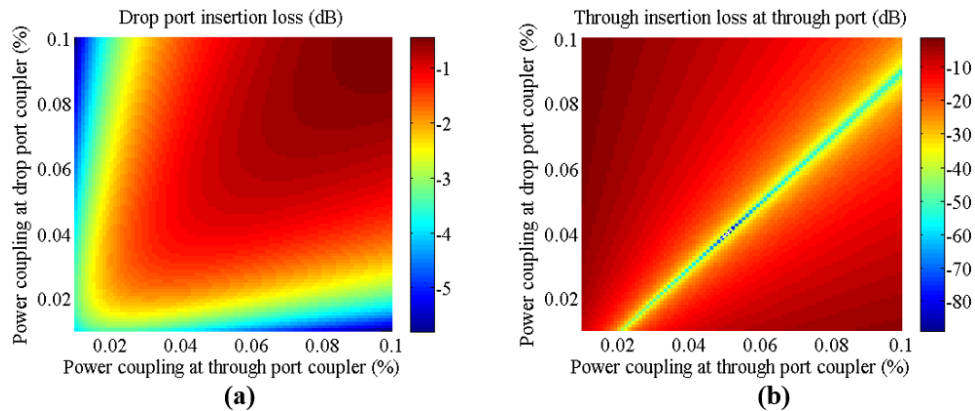


Fig. 6. (a) Drop port insertion loss in dB of a ring filter (i.e. from the SOA to the rear mirror in Fig. 4(a)). (b) Through port insertion loss in dB (i.e. from the SOA to the P-PD in Fig. 4(a)). Assumes 1dB/cm propagation loss, 25 μ m ring radius.

range (FSR) to a point where it is not reasonable to integrate both narrow band (low grating strength, κ) and high reflectivity (longer length) mirrors. Therefore a ring filter is needed to prevent mode-hopping observed in previous implementations of DBR lasers. Figure 3(b) show such a filtered mirror response. The DBR bandwidth requirement is therefore loosened to the channel spacing less any fabrication variation inherent in the technology used to create the athermal grating rather than something as narrow as the laser FSR. Designing the ring filter for this cavity requires a ring with a bandwidth on the order of the FSR of the cavity and a tuning range on the order of the bandwidth of the DBR. The ring's FSR can be smaller than the channel spacing and is ideally slightly less than the DBR bandwidth. The coupler designs can be made utilizing Fig. 6.

As is clear from Fig. 6(a), a symmetric design where both through and drop couplers are identical is preferred for lowest total laser loss with the ring as an intracavity element, as in Fig. 4(a). There is a little bit of flexibility in adding an asymmetry in the coupler design without a large variation in drop port insertion loss, however you can stumble into (or near) the quasi-critical coupling region denoted by the sharp increase in through port insertion loss in Fig. 6(b), which will block the through port transmission to a monitor PD. As is clear from Fig. 6(a), this through port critical coupling regime doesn't significantly change the intracavity laser loss, just the ratio of power out of the multiple outputs of the laser cavity. Therefore the additional energy is lost in radiation out of the ring.

Finally, an additional example is shown in Fig. 7 with an integrated wavelength locker. This wavelength locker uses a quarter wavelength shifted DBR as a filter to the input of the integrated wavelength monitor photo-diode. Utilizing either a wavelength operation point on the steep section of the high transmission notch or the maxima of this notch to reduce back reflections into the laser, a dither can be added to a phase section of the tunable laser to make a signal for the monitor diode which can be interpreted through the PID controller on the co-packaged Tx driver board or integrated into the SOI fabrication itself. Equivalently, another athermalized filter such as a high-Q resonator or integrated athermal FP cavity could work, however, an athermal grating is used for this filter because it has a higher fabrication tolerance to hit a precise wavelength than other filters such as rings. This tolerance can reduce or eliminate the need for post-fabrication trimming.

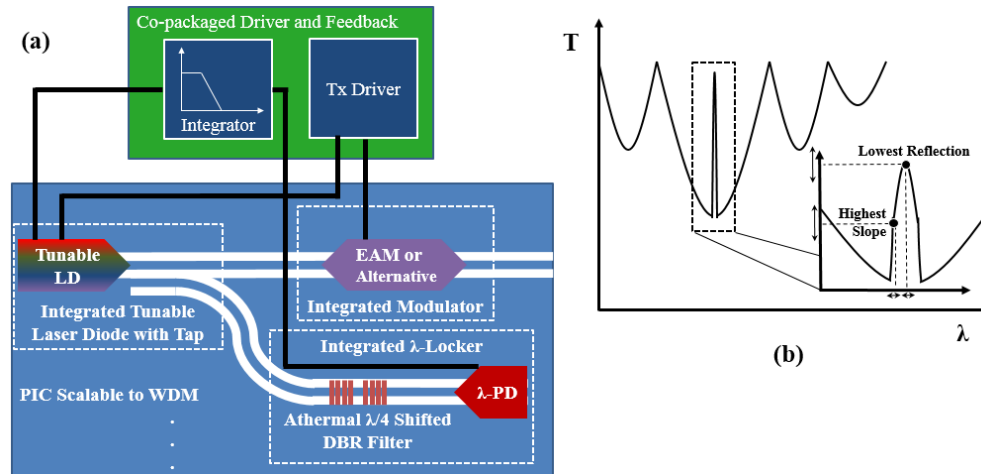


Fig. 7. (a) Schematic of an integrated transmitter with on-chip wavelength locker utilizing a quarter wavelength shifted DBR as a filter to an integrated monitor photodiode. This is co-packed with the control electronics. (b) the transmission of the wavelength locker filter concept is plotted with a slight wavelength dither on the high slope and lowest reflection of the filter notch caused by the $\lambda/4$ shift.

4. Summary and conclusions

An argument for targeting denser uncooled channel spacing was made followed by a review of how to achieve this with athermal designs. A simple athermal circuit concept implementable in MZIs and AWGs on most platforms is reviewed and shown to be limited for IIR filters, such as rings and DBRs. Therefore, materials based athermal waveguides are presented as an alternative to overcome such limitations with a brief theoretical description. The presence of SiO_2 lower cladding in SOI enables increased confinement in a negative TOC material top cladding of a Si core waveguide, making it possible to achieve both zero and negative waveguide TOCs. Therefore, athermal laser designs based on a modification of the Hybrid Silicon Laser are proposed to utilize such athermal waveguides without the use of external wavelength lockers required for conventional tunable lasers solutions. These proposed designs encompass entirely passive athermalization, and simple feedback loops with passively athermalized integrated reference filters using athermal DBR gratings. We project that such designs will provide the basis for a new class of uncooled lasers for photonic integrated transmitters.

Acknowledgments

The authors acknowledge Chong Zhang for helpful discussions on details of this paper and support from Google for funding this research.